Insights into mechanochemical reactions at the molecular level: Simulated indentations of aspirin and meloxicam crystals

Michael Ferguson,[a,b] M. Silvina Moyano,[a] Gareth A. Tribello,[c] Deborah E. Crawford,[b] Eduardo M. Bringa,[d] Stuart L. James,*[b] Jorge Kohanoff,*[c] and Mario G. Del Pópolo*[ac]

a Dr. M. Ferguson, Ms. M. S. Moyano, Prof. M. G. Del Pópolo
CONCIET & Facultad de Ciencias Exactas y Naturales, Universidad Nacional de Cuyo, Mendoza, Argentina.
mdelpopolo@fcen.uncu.edu.ar

b Dr. M Ferguson, Dr. D. E. Crawford, Prof. S. L. James
School of Chemistry and Chemical Engineering, Queen's University Belfast, Belfast, Northern Ireland.
s.james@qub.ac.uk

c Dr. G. A. Tribello, Prof J. Kohanoff, Prof. M. G. Del Pópolo
Atomistic Simulation Center, School of Maths and Physics, Queen's University Belfast, Belfast, Northern Ireland
j.kohanoff@qub.ac.uk

d Prof. E. M. Bringa
CONICET & Facultad de Ingeniería, Universidad de Mendoza, Mendoza, Argentina

Table of Contents

1) Validation of the Force Field

We tested the force field (FF) models used in this work by comparing the values of selected physical properties calculated with them with those obtained from *ab initio* calculations performed with the plane wave DFT code, Quantum Espresso (QE).[1] Structural optimisations were performed using the PBE functional[2] with DFT-D2 corrections[3], ultrasoft pseudopotentials[4] and a plane wave energy cutoff of 70Ry. The Brillouin zone was sampled using the method developed by Monkhorst and Pack.[5] Table S1 shows that the FF gives values for the density and unit cell volume of aspirin and meloxicam that are in close agreement with the experimental values. The bulk moduli calculated with the force field are overestimated slightly, but this is not unprecedented for molecular crystals.[6] The cohesive energies and surface energies compare well with those obtained with DFT, however, and we are thus confident that this FF was sufficiently accurate to be used in the remainder of the investigation.

Table S1. Physical properties of aspirin and meloxicam calculated using the force field of this work (FF), as compared to the values obtained from DFT and the experimental information (EXP) available. [7] The units are as follows; volume ($Å^3$), density (gm^{-3}), bulk modulus (GPa), formation energy (kcal mol^{-1}) and surface energy (Jm^{-2})

	Aspirin			**Melxociam**		
Property	FF	DFT	EXP	FF	DFT	EXP
Density	1.42	1.51	1.40	1.58	1.66	1.57
Volume	842.36	794.50	854.30	737.80	702.85	742.51
Bulk Modulus	13.51	12.57	7.77	18.22	14.10	-
ΔE_{form}	-31.45	-32.58	-	-41.34	-38.63	-
$\Delta E_{surf}(100)$	0.11	0.09	0.08†	0.11	0.09	-
$\Delta E_{surf}(010)$	0.22	0.19	-	0.21	0.20	-
$\Delta E_{surf}(001)$	0.09	0.08	0.10†	0.12	0.10	-

†Values taken from the acid-base approach.[7]

2) Simulation Snapshots and Molecular Density Histograms

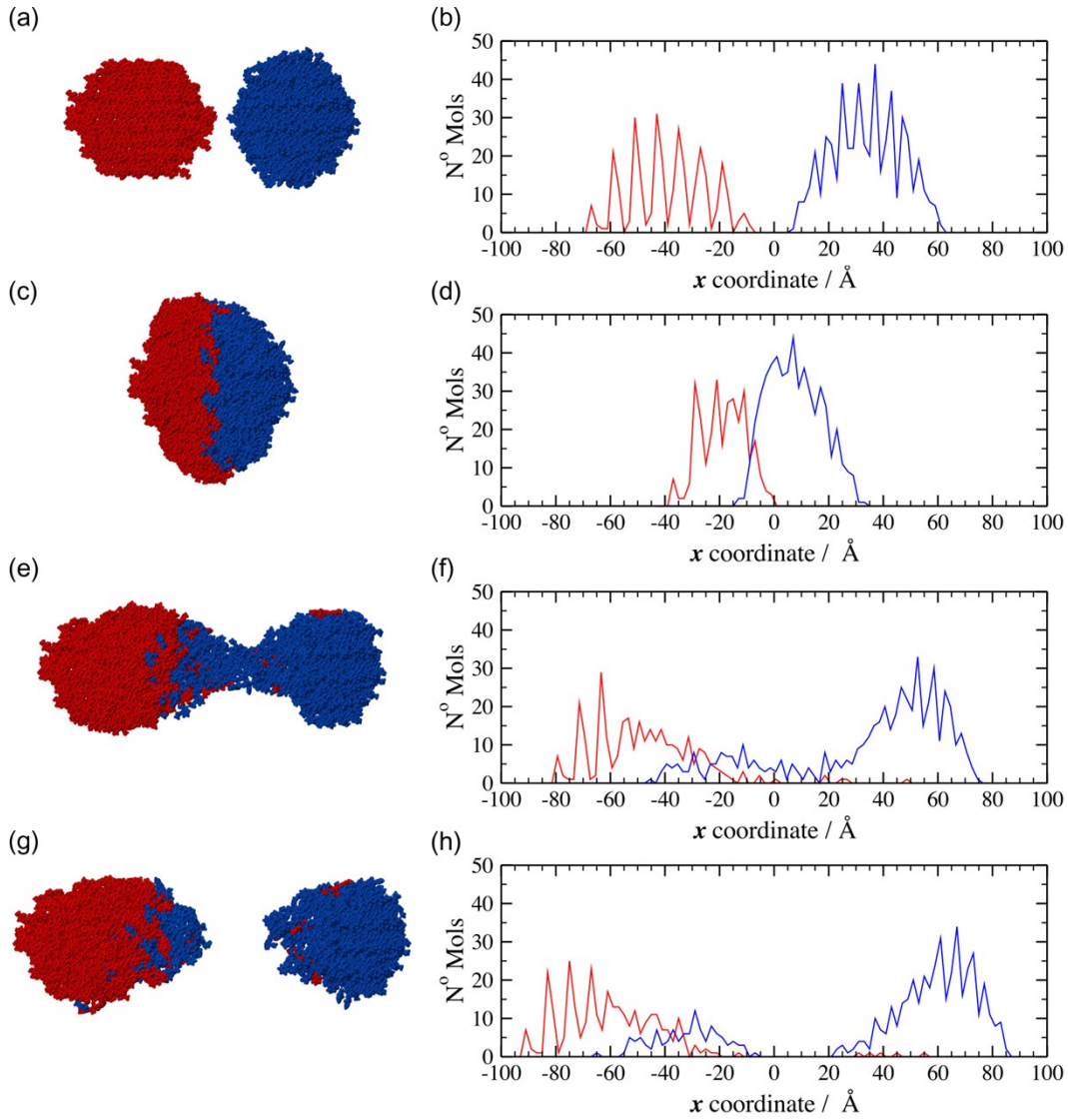

Figure S1. Left: snapshots of a simulated indentation between spherical clusters of meloxicam (red) and aspirin (blue) in configuration II, (a) Stage **1**: initial positions, (c) Stage **2**: point of maximum indentation, (e) Stage **3**: an intermediate stage during sphere retraction before the connective neck breaks up and (g) Stage **4**: resulting configuration after complete retraction. The clusters in this trajectory travelled with velocities of $4ms^{-1}$. Right: the distribution of molecules of meloxicam (red) and aspirin (blue) at stages **1**, **2**, **3**, and **4** for (b), (d), (f) and (h) respectively.

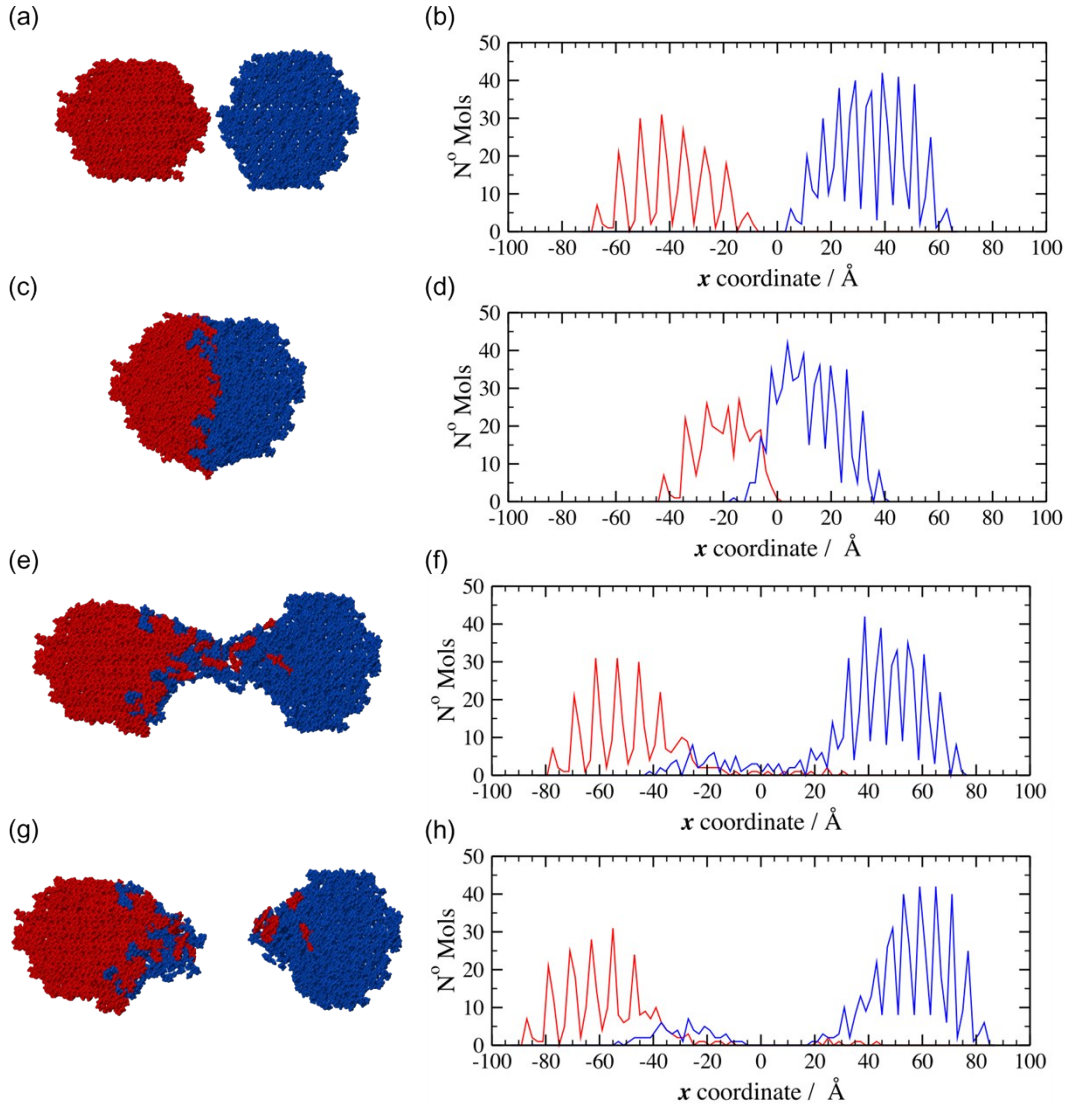

Figure S2. Left: snapshots of a simulated indentation between spherical clusters of meloxicam (red) and aspirin (blue) in configuration III, (a) Stage **1**: initial positions, (c) Stage **2**: point of maximum indentation, (e) Stage **3**: an intermediate stage during sphere retraction before the connective neck breaks up and (g) Stage **4**: resulting configuration after complete retraction. The clusters in this trajectory travelled with velocities of 4ms^{-1}. Right: the distribution of molecules of meloxicam (red) and aspirin (blue) at stages **1**, **2**, **3**, and **4** for (b), (d), (f) and (h) respectively.

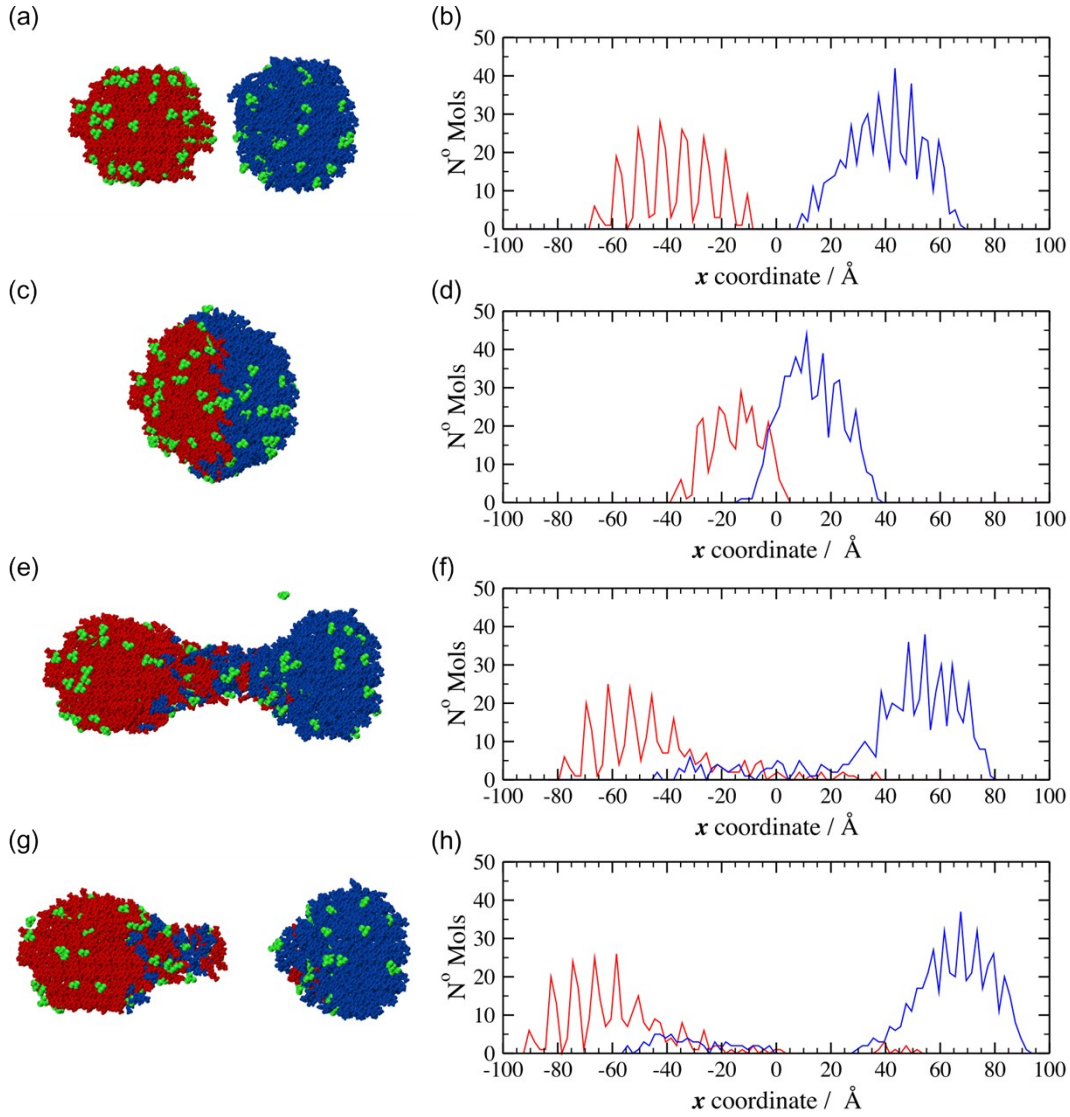

Figure S3. Left: snapshots of a simulated indentation between spherical clusters of meloxicam (red) and aspirin (blue) in configuration IV, partially solvated with 0.235 mol equiv. of $CHCl_3$ (green), (a) Stage **1**: initial positions, (c) Stage **2**: point of maximum indentation, (e) Stage **3**: an intermediate stage during sphere retraction before the connective neck breaks up and (g) Stage **4**: resulting configuration after complete retraction. The clusters in this trajectory travelled with velocities of $4ms^{-1}$. Right: the distribution of molecules of meloxicam (red) and aspirin (blue) at stages **1**, **2**, **3**, and **4** for (b), (d), (f) and (h) respectively.

3) Force Development During Indentation and Retraction

Further analysis followed that of previous works in indentation simulations, such as that of Landman *et al.* and other studies which concern atomic force microscopy (AFM) tips indenting surfaces.[8] In that, we recorded the development of the force in the direction of the indentation, with respect to both spheres simultaneously. This was achieved by calculating the average force along *x* experienced by the molecules with fixed positions at the rear of the clusters, on a per atom basis. The force was plotted versus the separation between the COM of the fixed layers of aspirin and meloxicam. Simulated indentations at lower rates naturally require longer simulation times and generate longer trajectories. Therefore, to retain consistency while reporting results, moving averages were applied to the raw data. The size of the moving average was set to the number of trajectory frames required for the COM separation to change by at least 2Å. As expected (Figures S4 – S7) the force development profiles for aspirin and meloxicam are almost mirror images of each other. The slight differences between the profiles are most likely determined by the size, shape and packing of the molecules of each species. The profiles follow the same pattern of events for the two species. At stage **1** (red dashed lines), the force response shows a small attractive force, due to the initial van der Waals interactions between the spheres. As the indentation process occurs and we approach stage **2** (green dashed lines), of the simulations, the magnitude of the force experienced along *x* increases to ~6nN. Upon the reversal of the spheres' velocities the force decreases in magnitude, more rapidly than it had increased and begins to fluctuate with a value close to zero. The fluctuation around zero remains present as the simulation passes through stage **3**, where the connective neck exists, and reaches stage **4**, (blue and purple dashed lines respectively), where the spheres become separate entities once again. The hysteresis of the force loop is common of indentations.[8] Marx et al. stated in a recent review paper[9] that forces on the sub-nN scale are not to be unexpected for intermolecular interactions such as hydrogen bonding. However, the review is generally focused on mechanochemical simulations of single molecules or one dimensional polymer chains rather than clusters. Therefore, while working with hundreds of molecules of aspirin and meloxicam whose crystalline structures each exhibit hydrogen bonding, we were not surprised to observe a greater magnitude in the force when the systems were stressed by the indentation process.

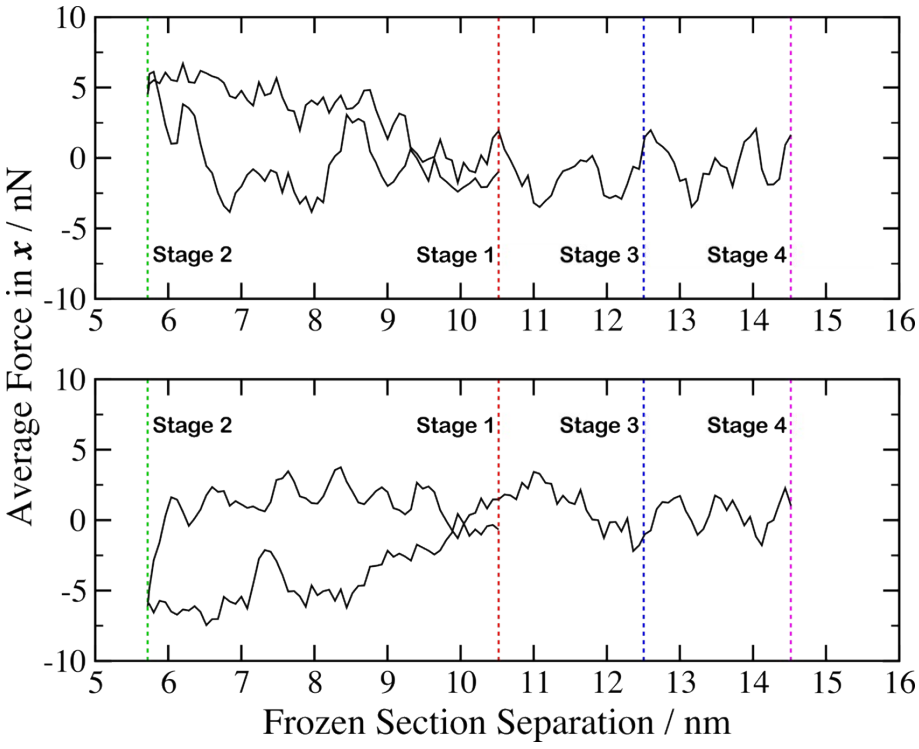

Figure S4. Plot of the development of the force experienced in the *x* direction by the sections of molecules of aspirin (top panel) and meloxicam (bottom panel), in configuration I, which had their trajectories fixed during a simulated indentation with sphere velocities of $4ms^{-1}$. The force experienced by these molecules at stages **1**, **2**, **3**, and **4** of the trajectory are signalled by the red, green, blue, and purple dashed lines respectively.

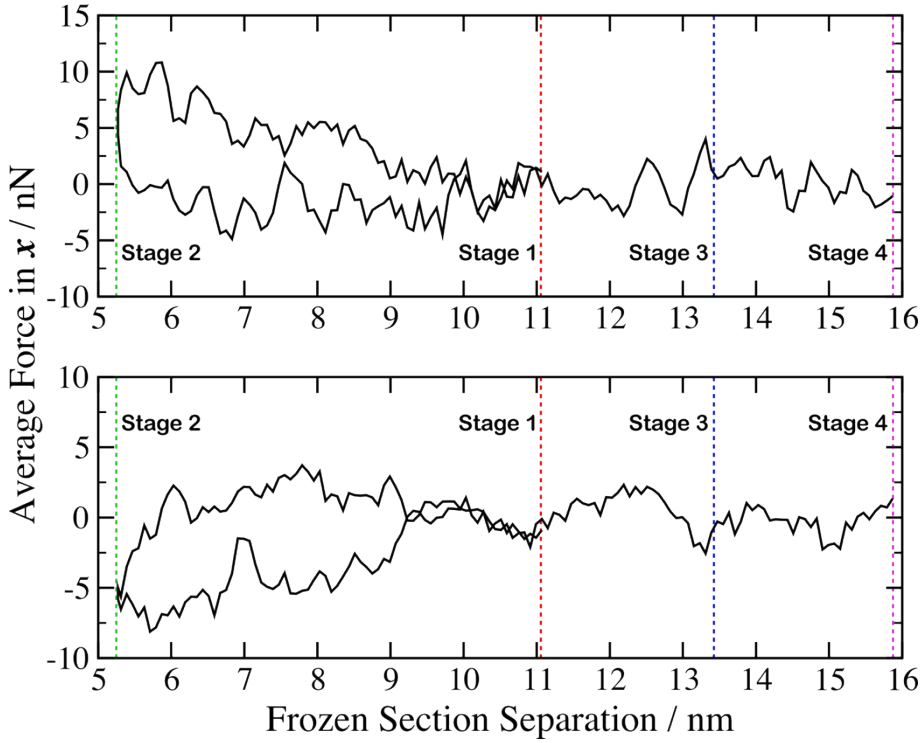

Figure S5. Plot of the development of the force experienced in the *x* direction by the sections of molecules of aspirin (top panel) and meloxicam (bottom panel), in configuration II, which had their trajectories fixed during a simulated indentation with sphere velocities of $4ms^{-1}$. The force experienced by these molecules at stages **1**, **2**, **3**, and **4** of the trajectory are signalled by the red, green, blue, and purple dashed lines respectively.

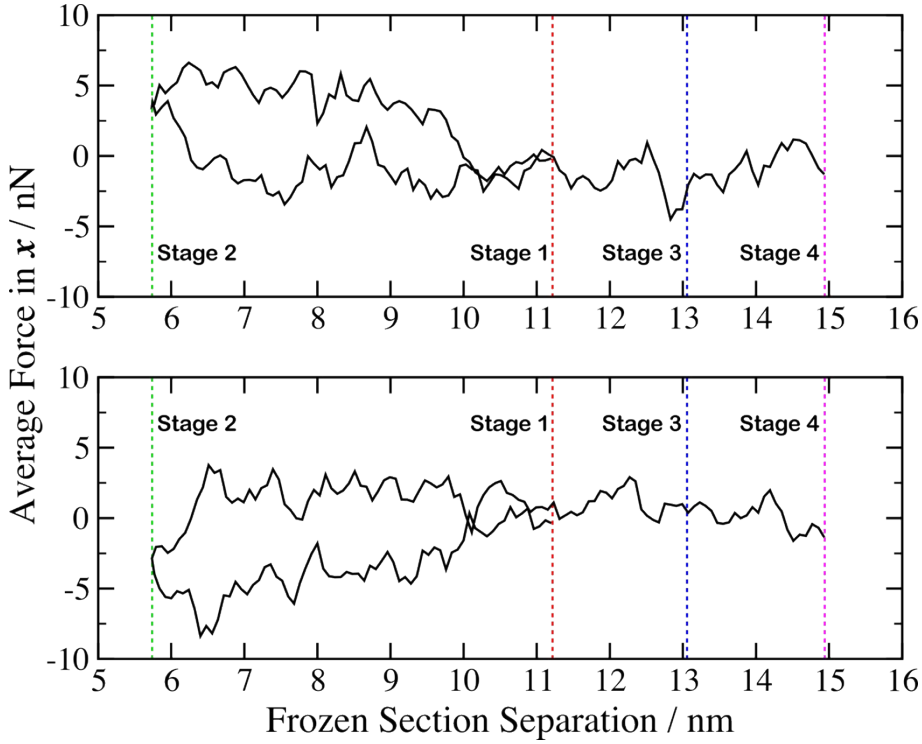

Figure S6. Plot of the development of the force experienced in the *x* direction by the sections of molecules of aspirin (top panel) and meloxicam (bottom panel), in configuration III, which had their trajectories fixed during a simulated indentation with sphere velocities of $4ms^{-1}$. The force experienced by these molecules at stages **1**, **2**, **3**, and **4** of the trajectory are signalled by the red, green, blue, and purple dashed lines respectively.

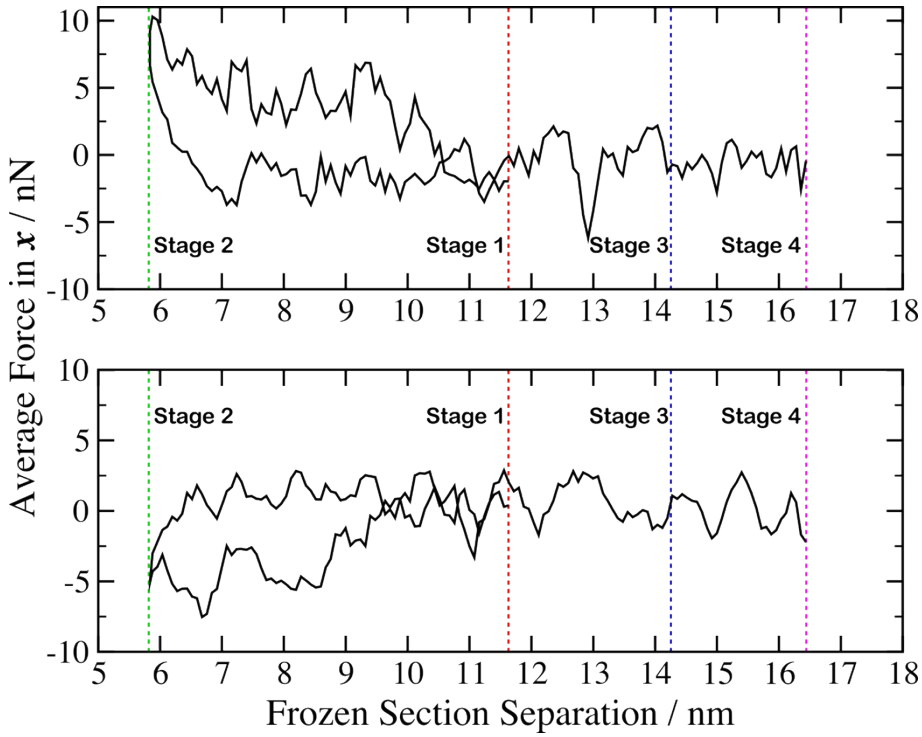

Figure S7. Plot of the development of the force experienced in the *x* direction by the sections of molecules of aspirin (top panel) and meloxicam (bottom panel), in configuration IV, which had their trajectories fixed during a simulated indentation with sphere velocities of 4ms^{-1}. The force experienced by these molecules at stages **1**, **2**, **3**, and **4** of the trajectory are signalled by the red, green, blue, and purple dashed lines respectively.

4) Transfer of Molecules Between Clusters and Connective Neck Analysis

Looking at stage **4** configurations, shown in Figures 2 (manuscript), S1, S2, and S3, it appears that, in general, a greater amount of aspirin is transferred than meloxicam. We therefore counted the total number of molecules transferred as a percentage of the number of molecules that were allowed to move during the simulation. The histograms for meloxicam (red) and aspirin (blue) at stage **4** configurations all show two distinct sections for each species. Therefore, both of the sections were integrated separately and the smaller resulting value gave the number of molecules transferred to the opposing species. The sum of these two numbers would therefore give the total number of molecules transferred during the simulation. The percentage transfer of molecules is calculated as follows;

$$\%_{Transfer} = \frac{N_{Trans}}{N_{Free}} \times 100$$

Where N_{Trans} and N_{Free} are the numbers of molecules that have been transferred and the number of mobile molecules.

Table S2. Total percentage transfers of aspirin and meloxicam molecules observed for simulated single indentations. Data for all configurations and indentation rates investigated.

Configuration	Indentation Rates / ms^{-1}			
	4.0	2.0	1.0	0.5
	Percentage Transfer / %			
I	9.94	8.66	19.32	17.61
II	16.90	15.20	21.45	14.49
III	10.42	8.25	9.41	10.56
IV	10.51	10.13	14.91	21.59

Connective Neck Analysis

The length of the connective neck, l_{cn}, was measured in terms of the position of the centre of mass (COM) of all the fixed aspirin and meloxicam molecules in the clusters. It was defined as,

$l_{cn} = d_4 - d_2$

where d_2 and d_4 are the separations between COM at stages **2** and **4** respectively. The values of l_{cn} for all of the simulations performed are reported in Table S3.

Table S3 Lengths of the connective necks formed between clusters of aspirin and meloxicam during the retraction stage of simulated indentations for all configurations and indentations rates investigated.

Configuration	Indentation Rates / ms^{-1}			
	4.0	2.0	1.0	0.5
	Connective Neck Length / nm			
I	8.66	8.40	8.34	9.14
II	10.76	10.76	9.74	8.30
III	8.91	8.71	8.12	8.30
IV	10.25	12.13	9.69	9.42

5) Local Heating Study

To test for the presence of localised areas of high temperature, we performed simulations of high energy impacts between a meloxicam cluster and the (100) surface of aspirin. The aspirin slab (3200 molecules) was generated from a 20x10x5 supercell which was annealed to half of the melting point for 0.25ns before equilibrating the system at 300 K for 1ns. The surface was subsequently opened and the system was equilibrated again at 300K for 1ns. The aspirin molecules that made the bottom layer of the slab were fixed in space. To measure the local temperature, the velocities of the aspirin molecules located within a hemisphere of 2.75nm diameter and centred on the slab surface (cyan region Figure S8) were monitored throughout the simulations. To complete the initial configuration for the impact (Figure S8) the meloxicam sphere (302 molecules) was placed above the slab, leaving a 5Å gap between the cluster and the aspirin surface.

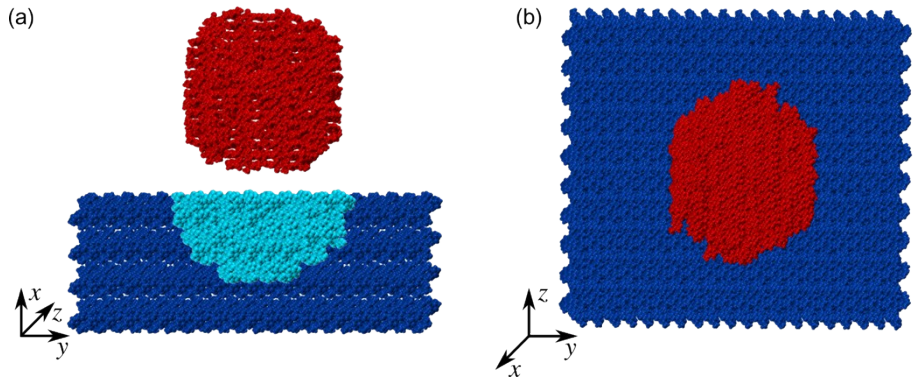

Figure S8. Images of final design of the system used to investigate the phenomenon of local heating between the (100) aspirin surface (blue) and the meloxicam sphere (red) from the perspectives of, (a) the side, showing the 5 Å separation between the two species and a cross-sectional view of the localised region of aspirin (cyan), and (b) the top, showing the centralised placement of the cluster over the surface.

High energy impacts were induced by augmenting the COM velocities of the molecules in the meloxicam sphere, to 8, 4 and 2ms^{-1}, in the *X*-direction at the beginning of the simulations. These simulations were performed in the microcanoncical (NVE) ensemble and allowed to develop for 1ns in order to monitor the temperature progression after the cluster-slab impact. The temperature profiles for each of these simulations is shown in Figure S9, in which both the local (green) and the slab (black) temperatures are plotted. The local temperature profiles show slight variations in temperature, however they are much lower than would be predicted according to the magma-plasma model.[10] The temperatures of the full aspirin slab show a small increase of ~2.5K, in each simulation, whereas the local temperature was more prone to fluctuations due the smaller number of molecules within the spherical region. For the simulation at 8ms^{-1}, for example, the impact occurs at 62.5ps which is not

evident in the temperature analysis (Figure S9, a). Instead the local temperature fluctuates around the temperature of the full aspirin slab, again showing an overall increase throughout the simulation. This remains true for the 4 and 2ms^{-1} simulations where the impacts occur at 125 and 250ps respectively. We decided to exaggerate the impact velocity and performed a simulation with an impact velocity of 32ms^{-1}, and again no significant rise in local temperature was observed (Figure S10). Finally, a control simulation was performed to confirm that the ~2.5 K increase in slab temperature in each simulation was a result of the collision and not a random fluctuation. The control simulation started from the same configuration as that of the impact simulations and, as expected the cluster did not impact the surface. Again, we monitored both the local, and slab temperatures for a period of 1ns. Figure S11 shows no increase in either the local or the slab temperatures, thereby confirming that the 2.5K increase observed previously was caused by the impacts.

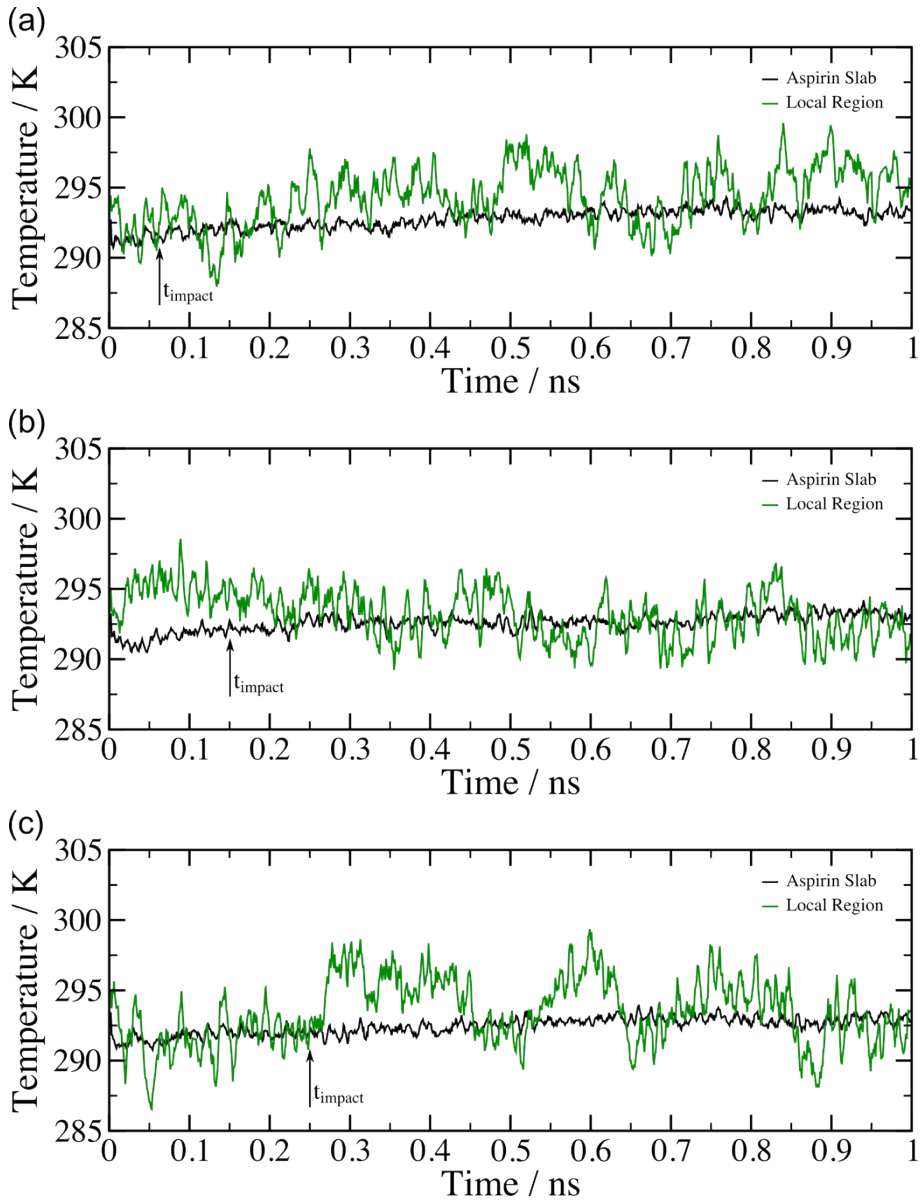

Figure S9. Plots comparing the temperatures of the aspirin (100) surface (black) and the localised region at the point of impact (green) for meloxicam cluster impact velocities of (a) 8ms^{-1}, (b) 4ms^{-1}, (c) 2ms^{-1}.

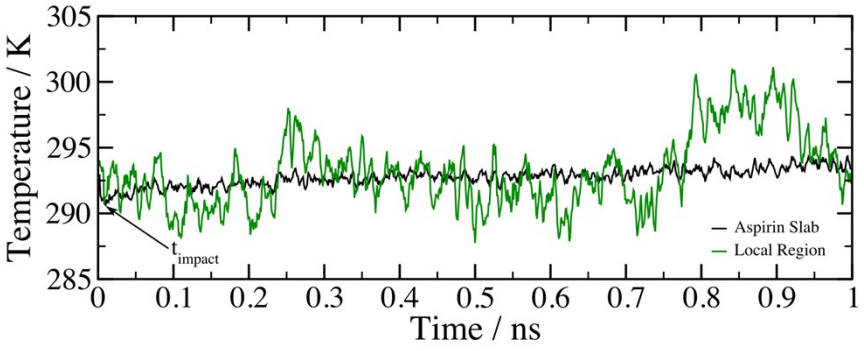

Figure S10. Plot comparing the temperatures of the aspirin (100) surface (black) and the localised region at the point of impact (green) for a meloxicam cluster impact velocity of 32ms^{-1}.

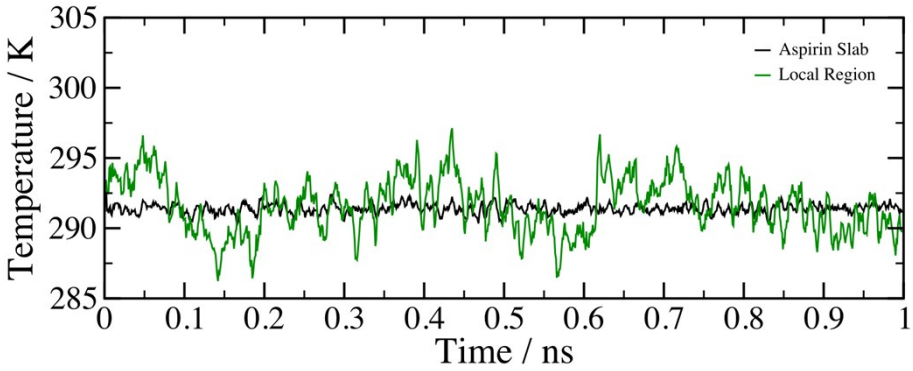

Figure S11. Plot comparing the temperatures of the aspirin (100) surface (black) and the localised region (green) when the meloxicam cluster does not impact against the surface.

6) References

1 P. Giannozzi, S. Baroni, N. Bonini, M. Calandra, R. Car, C. Cavazzoni, D. Ceresoli, G. L. Chiarotti, M. Cococcioni, I. Dabo, A. Dal Corso, S. de Gironcoli, S. Fabris, G. Fratesi, R. Gebauer, U. Gerstmann, C. Gougoussis, A. Kokalj, M. Lazzeri, L. Martin-Samos, N. Marzari, F. Mauri, R. Mazzarello, S. Paolini, A. Pasquarello, L. Paulatto, C. Sbraccia, S. Scandolo, G. Sclauzero, A. P. Seitsonen, A. Smogunov, P. Umari and R. M. Wentzcovitch, *J. Phys. Condens. Matter*, **2009**, 21, 395502.

2 J. P. Perdew, K. Burke and M. Ernzerhof, *Phys. Rev. Lett.*, **1996**, 77, 3865–3868.

3 S. Grimme, *J. Comput. Chem.*, **2006**, 27, 1787–1799.

4 A. M. Rappe, K. M. Rabe, E. Kaxiras and J. D. Joannopoulos, *Phys. Rev. B*, **1990**, 41, 1227–1230.

5 H. J. Monkhorst and J. D. Pack, *Phys. Rev. B*, **1976**, 13, 5188–5192.

6 R. Faccio, P. a. Denis, H. Pardo, C. Goyenola and A. W. Mombrú, *J. Phys. Condens. Matter*, **2009**, 21, 285304.

7 Y. Kim, K. Machida, T. Taga and K. Osaki, *Chem. Pharm. Bull.*, **1985**, 33, 2641–2647; G. F. Fabiola, V. Pattabhi, S. G. Manjunatha, G. V. Rao and K. Nagarajan, *Acta Crystallogr. Sect. C Cryst. Struct. Commun.*, **1998**, 54, 2001–2003; A. M. Reilly and A. Tkatchenko, *Phys. Rev. Lett.*, **2014**, 113, 1-5; J. Y. Heng, A. Bismarck, A. F. Lee, K. Wilson and D. R. Williams, *J. Pharm. Sci.*, **2007**, 96, 2134–2144.

8 U. Landman, W. Luedtke and E. Ringer, *Wear*, **1992**, 153, 3–30; C. J. Ruestes, E. M. Bringa, Y. Gao and H. Urbassek, in *Applied Nanoindentation In Advanced Materials* (Eds.: A. Tiwari, and S. Natarajan), Wiley-Blackwell, **2017**; K. Komvopoulos and W. Yan, *J. Appl. Phys.*, **1997**, 82, 4823–4830.

9 J. Ribas-Arino and D. Marx, *Chem. Rev.*, **2012**, 112, 5412-5487.

10 P. Baláž, *Mechanochemistry in Nanoscience and Minerals Engineering*, Springer Berlin Heidelberg, Berlin, **2008**; P. Baláž, M. Achimovičová, M. Baláž, P. Billik, Z. Cherkezova-Zheleva, J. M. Criado, F. Delogu, E. Dutková, E. Gaffet, F. J. Gotor, R. Kumar, I. Mitov, T. Rojac, M. Senna, A. Streletskii and K. Wieczorek-Ciurowa, *Chem. Soc. Rev.*, **2013**, 42, 7571–7637.